Cool Stars, Stellar Systems and the Sun
ASP Conference Series, Vol. 154, 1998
eds. R. A. Donahue and J. A. Bookbinder

Surface Imaging by Microlensing

Dimitar D. Sasselov

Harvard-Smithsonian Center for Astrophysics, Cambridge, MA 02138, USA

Abstract:

Gravitational microlensing is a new technique for studying the surfaces of distant stars. A point mass lens, usually a low-mass star from the disk, will typically resolve the surface of a red giant in the Galactic bulge, as well as amplify its brightness by a factor of 10 or more. Such events are now detected in real time and can be followed up with precision photometry and spectroscopy. The motivation for stellar imaging via microlensing lies in its unique ability to provide center-to-limb variation of spectral diagnostic lines. Such variation maps into a variation with depth in the stellar atmosphere — a unique and very valuable constraint for modeling the structure of red giants' atmospheres. We illustrate the technique on a recent successful observational campaign and discuss the implications for current stellar models.

1. Introduction

Gravitational microlensing is a new technique for studying the surfaces of distant stars (Sasselov 1996, 1997a), which is observationally viable for red giants in the Galactic bulge (Alcock et al. 1997). Microlensing events have typical durations of weeks to months. While most lenses are point masses, many ($\sim 20\%$) of the sources monitored in the Galactic bulge are red giants and supergiants — their angular radii are *comparable* to the Einstein radius of a sub-solar mass lens (in the range of 50μas). In addition to being resolved by most lenses, the projected disks of bulge giants are large enough to make the probability for a lens transit very high — in fact, at least one such event (MACHO Alert 95–30) was very well observed recently (Alcock et al. 1997), and two near misses occured this summer (MACHO Alert 97–BLG–10 & 97–BLG–56).

We study stars by the radiation emergent from their surface layers. While the theory of numerical radiative transfer has made great progress over the last decade, its application to stellar atmospheres has been, for the most part, limited to one-dimensional equilibrium models. One reason was, partly, because of technology — we were unable to observe directly the surfaces of other stars. Stellar interferometry, eclipsing binaries, and Doppler imaging, provide valuable surface information, like limb darkening and stellar spots. However, by its nature, microlensing imaging allows us to observe the center-to-limb variation in spectral lines (and their profiles). Such observations are invaluable for the construction of detailed models of the atmosphere, as it has been long known from the study of the Sun. The solar disk brightness distribution as a function of wavelength has been mapped into the depth distribution of temperature and density, which allows a complete synthesis of the observed solar spectrum (Kurucz 1990). The situation with stars has been confined to very much lower accuracy; the data cannot be used to build a model atmosphere, as in the case of the Sun.

The 2-D and 3-D structure of stellar atmospheres other than the Sun is not well known. Theoretical modelling relies heavily on the solar atmosphere model (Nordlund & Dravins 1990), but this situation is unfortunate for a number of reasons. There has been an increased demand for accurate stellar models from a number of fields, especially regarding red giants and supergiants. Our Sun is not a good zero point for most of these applications.

2. Gravitational Microlensing as a Stellar Microscope

The amplification of a point source by a point mass, M, depends only on their projected separation d (Paczyński 1986),

$$A(d) = \frac{d^2 + 2}{d(d^2 + 4)^{1/2}}, \tag{1}$$

where d is expressed in units of the angular radius of the Einstein ring of the lens, $\theta_E = ([4GM/c^2][D_{\rm LS}/D_{\rm OL}D_{\rm OS}])^{1/2}$, and $D_{\rm OL}, D_{\rm LS}$, and $D_{\rm OS}$ are the distances between the observer, lens and source. The total flux received from an extended source is therefore obtained by integration over its infinitesimal elements,

$$F(t) = \int_0^{\tilde{R}_s} r dr B(r) \int_0^{2\pi} d\theta A(d), \tag{2}$$

where $B(r)$ is the surface brightness profile of the source in the projected polar coordinates (r, θ) around its center. For simplicity, we assume that the stellar emission is circularly symmetric, although this is not a limitation (see Heyrovsky & Loeb 1997; Heyrovsky, Loeb, & Sasselov 1997), and denote the source radius by $R_s = \tilde{R}_s \times (\theta_E D_{\rm OS})$. All projected length scales are normalized by the Einstein ring radius. Using the law of cosines

$$d = |\vec{d_0} - \vec{r}| = (d_0^2 - 2d_0 r \cos\theta + r^2)^{1/2} \ , \tag{3}$$

where $d_0 = (b^2 + v^2 t^2)^{1/2}$ is the projected separation between the lens and the source center, b is the projected impact parameter of the source center, v is the transverse velocity of the lens in units of $\theta_E D_{\rm OL}$, and $t = 0$ is the midpoint time of the lensing event. For a circularly symmetric source, the resulting light curve is time-symmetric with $F(t) = F(-t)$.

As a result of this dependence on $B(r)$, when the source is resolved, $F(t)$ is wavelength dependent through $B(r)$, despite the achromatic nature of gravitational lensing. For example, in the optical continua, $B(r)$ will reflect the wavelength dependence of limb darkening, hence broad-band photometry will show chromaticity due to that effect (Gould & Welch 1996; Heyrovsky, Loeb, & Sasselov 1997; Valls-Gabaud 1997). Narrow-band photometry could reveal resonant line emission in cool giants in a much more dramatic ways, as shown by Loeb & Sasselov (1995). And finally, high-resolution spectra will reveal spectral line profile changes with time, representing the subtle center-to-limb variation of different atomic and molecular transitions.

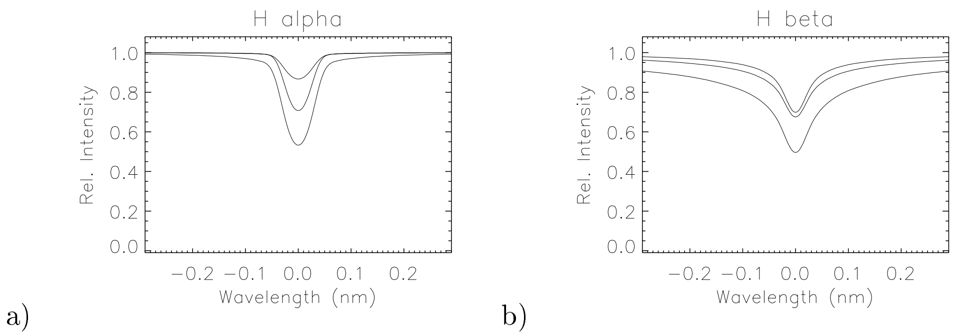

Figure 1. Line profiles at three different viewing angles (characterized by their cosines μ) on the stellar disk from the non-LTE model of the M95–30 red giant (Sasselov 1997a). a) Three profiles of the hydrogen Hα line from disk center at μ=0.98 (bottom), through μ=0.5, to very near the limb at μ=0.02 (top). b) Same for the hydrogen Hβ line. Note the difference in profile shape between the two lines, *as well as* their change with μ.

3. Probing the Atmospheres of Red Giants

3.1. Stellar Microscopy

Stellar disks are projected hemispheres, which implies an axisymmetric variation of the intensity with position as it maps into a variation with depth. In general, the emergent continuum radiation at the center of the disk is formed deeper than the radiation we see near the limb. Over a very wide spectral range for stars of different temperature, the center-to-limb variation of the continuum emission is manifested as limb darkening. Unlike continuum radiation, spectral lines provide a larger choice of center-to-limb variations. In the majority of stars we deal with absorption lines of different strength, arising from atomic or molecular bound-bound transitions. Most moderately strong and weak lines diminish towards the limb (Figure 1). This variation could be observed in a microlensing event by measuring the total equivalent widths of spectral lines on medium-resolution spectra with high S/N (as shown in Figure 3), or directly — on high-resolution spectra. The change of the Hα line seen in Figure 3, reflects the expected change in the line at different viewing angles — strong at disk center (lens position 0.0) and weak at disk limb (lens position 1.0).

The variation of intensity from disk center to disk limb is studied theoretically by computing the contribution function of each transition; a function which defines the line forming region in space (i.e., depth in atmosphere) and frequency. Here we define (see Magain 1986) the non-LTE contribution function, CF, for the relative line depression, as:

$$\mathrm{CF}(\log\ \tau_0) \;=\; \frac{\ln\ 10}{\mu}\tau_0\frac{\kappa_\mathrm{l}}{\kappa_0}\Big(1-\frac{S_\mathrm{l}}{I_\mathrm{c}}\Big)e^{-\tau_\mathrm{R}/\mu},$$

where τ_0 is the optical depth at a reference wavelength λ_0, τ_R is defined in terms of $\kappa_\mathrm{R} = \kappa_\mathrm{l} + \kappa_\mathrm{c} S_\mathrm{c}/I_\mathrm{c}, \kappa_0$ is the absorption coefficient at λ_0, κ_l and κ_c are the line

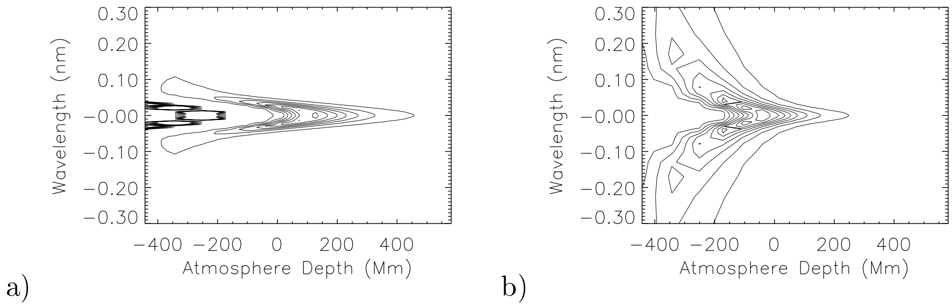

Figure 2. Line forming regions, represented by the CFs, of the hydrogen Hα and Hβ lines shown in Figs.1ab. The contribution functions (CFs) are in units of intensity and are angle averaged. a) The hydrogen Hα line is formed higher in the atmosphere overall, especially its line core. b) The hydrogen Hβ line is formed deeper and has well developed wings. However, due to the background line and continuum opacity these line wings will not be visible at small viewing angles. Both lines will have strong, but different, center-to-limb variation.

and continuum absorptions, respectively, $S_{\rm l}$ and $S_{\rm c}$ are the line and continuum source functions, respectively, $I_{\rm c}$ is the emergent continuous intensity (if the line were absent), and $\mu = \cos\,\theta$. The traditional dependence on frequency has been omitted from our notation for simplicity. The CF for a given synthesized spectral line will indicate where the line is formed; i.e., the line forming region, and consequently, at what velocity. We show the CFs for two hydrogen lines in our M95–30 model in Figure 2.

Microlensing suffers from some of the same degeneracies inherent to Doppler imaging, namely with respect to the lens path. It could be overcome in the coming years with microlensing parallax observations (using spacecraft on the Earth orbit). However, unlike Doppler imaging, line profile changes are easy to measure and interpret. Of course, the rate of rotation is of no importance to microlens imaging — in fact, microlensing can be used to determine $v\sin i$ independently (Maoz & Gould 1994) from the Doppler shifts of the spectral lines.

In order to explore the complete optical spectrum of a lensed star with all necessary detail, one needs a very fast code which "microlenses" all frequencies/wavelengths of an extended source as a function of time. Such an efficient method was developed by Heyrovsky & Loeb (1997), Heyrovsky, Loeb, & Sasselov (1997), and is used in the calculations of Figure 3.

By now there are more than 150 microlensing events detected towards the Galactic bulge by the MACHO and OGLE2 projects. The standard light curve of an event is characterized by two observables: its peak amplitude and duration (Paczyński 1986). Finite-size effects arise from resolved features on the surface of the lensed star. Finite-size effects have been studied as methods to partially remove the degeneracy of microlensing light curves through the alterations of the standard light curve (Nemiroff & Wickramasinghe 1994; Gould 1994, 1995; Witt & Mao 1994; Gould & Welch 1996), its polarized emission (Simmons, Newsam,

& Willis 1995), spectral shifts due to stellar rotation (Maoz & Gould 1994), and narrow-band photometry in resonance lines (Loeb & Sasselov 1995). Here we want to put the emphasis on the inverse problem, that of stellar microscopy — reconstructing the stellar surface features and probing the stellar atmosphere.

Red giants comprise a major component of the stars that are being monitored in the bulge by the microlensing surveys. For example, in the OGLE dataset about 19% of all the stars have radii $\gtrsim 5R_\odot$ (Loeb & Sasselov 1995). Therefore, for $D_{\rm OL} = 6$ kpc, the fraction of giant lensing events with $b < \tilde{R}_s$ (when the lens transits across the disk of the source star) is of order $\langle \tilde{R}_s \rangle \approx 4\% \times (M/0.1M_\odot)^{-1/2}$. This is a large fraction, and observations are additionally aided by the intrinsic brightness of the giants.

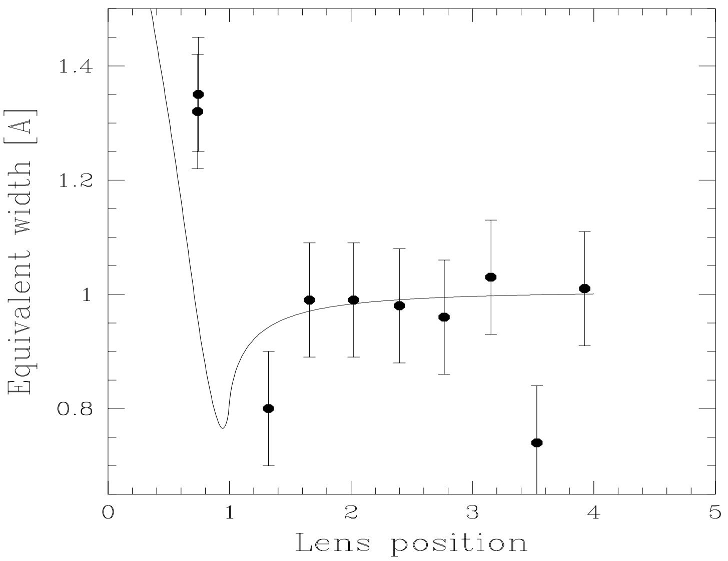

Figure 3. The theoretical model variation of the Hα line (solid line) compared to the observed variation (equivalent width) in M95–30 by Alcock et al. (1997). Unfortunately, there were no observations made near the limb crossing nights (lens position 1.0). The error bars may be an underestimate, given the quality of the spectra and the confused spectral reagion around the Hα line. The observations between lens positions 1.0 and 4.0 were obtained on 8 consecutive nights (from Heyrovsky, Sasselov, & Loeb 1997).

Stellar microscopy can constrain dramatically models of giant atmospheres by providing center-to-limb variations of different line profiles in the spectra of bulge red giants. Gravitational microlensing offers an easily accessible, immediate, and inexpensive way to image at least some types of stars. It also offers access to stellar populations (in the Galactic bulge and Magellanic Clouds), which are beyond the reach of any interferometer. Gravitational lensing does resolve, *as well as* amplify, thus making 17 *mag* bulge giants as bright as 12 *mag* — a target easily accessible to echelle spectrographs.

There is already a proof-of-concept result, based on the spectroscopy obtained by the MACHO-GMAN collaboration (Alcock et al. 1997) of event M95–30. Our 1-D model of the lensed red giant in that event reproduces well the observations of the Hα line shown in Figure 3, as well as the TiO bands and the photometry (Heyrovsky, Sasselov, & Loeb 1997). We are currently working on the high-quality spectra of M95–30 obtained by Alcock et al. (1997) to improve the model.

3.2. Challenges in Modelling of Cool Giants

Red giants are a major component of any galactic stellar population. The parameters of the red giant branch are derived from multi-color photometry interpreted with stellar atmosphere models (e.g., Vandenberg & Bell 1985; Kurucz 1992). Such model atmospheres are one-dimensional integrations in semi-infinite slabs in hydrostatic and radiative equilibrium. Many problems and the need to improve these models were reviewed recently by Kurucz (1997). Many assumptions and simplifications are being made — some of them have not been verified by direct observations. Such examples are the treatment of convective transport and small-scale velocity fields (e.g., micro- and macro-turbulence).

In traditional one-dimensional radiative transfer modeling one usually parameterizes small-scale dynamic motions with an assumed microturbulent velocity distribution. Small-scale in this case refers to motions that occur within a photon mean free pathlength, so that these motions contribute to the intrinsic broadening of the line profile. On top of these small-scale motions there are motions on larger scales that have to be accounted for in observations with limited spatial resolution. These are often called macroturbulence, which is a mis-characterization, since most of these motions occur in well organized forms like radial- and non-radial pulsations, and convective flows. Macroturbulence is applied as additional broadening to the emergent line profiles. As such it has no consequences for the radiative transport and energy balance in the atmosphere. Microturbulent broadening, on the other hand, does affect the flow of radiation through the stellar atmosphere because they provide additional line opacity.

Although one-dimensional models exist for stars with a wide variety of effective temperatures and gravities (e.g., the Kurucz 1992 models or the Allard & Hauschildt 1995 models for later type stars) little modeling has been done of the multi-dimensional structure of stars other than the Sun (Dravins 1990), and practically none for red giants. The stellar evolution models on the other hand are dependent on a number of parameters, which describe poorly understood physics, e.g., the treatment of convection near the surface of the star. Using scaling arguments, Schwarzschild (1975) suggested that red giants may have only a small number of very large convection cells on their surface. High-resolution microlensing data can provide insights into these issues and help develop efficient and physically consistent recipes for calculating small-scale velocity fields. For example, assuming that small-scale velocity fields are well represented by a turbulent spectrum one could model the depth-dependent microturbulent velocity with a simple self-consistent model of turbulence in the spirit of Canuto, Goldman, & Mazzitelli (1996), and treat the subgrid cascade. It is clear, however, that a 3-D transfer calculation is necessary to provide the initial spectral scales for such a scheme (Sasselov 1997b).

Problems such as described above have hindered significant improvement in the determination of fundamental stellar properties over the past 20 years. Just to illustrate one of the current problems involving red giants calibrations, consider the "age of the Universe" debate. Calculating isochrones for globular clusters — using the same evolutionary models and assumptions, but different model atmospheres for $T_{\rm eff}$ and bolometric correction calibrations (Bell-Gustafsson vs. Kurucz), leads to a 20% difference in age estimates (Salaris et al. 1997; Vandenberg 1997). Given the conflicting results in interpreting the *Hipparcos* satellite data on subdwarf calibrations of globular cluster sequences (Reid 1997; Pont 1997), the issue of isochrone calibration remains open and very important. The need for 2-D and 3-D tools for atmosphere modelling comes also from recent successful direct stellar imaging with the Hubble Space Telescope (e.g., Uitenbroek, Dupree, & Gilliland 1998).

4. Conclusions

Gravitational microlensing offers unique ways to: 1) study the depth dependence in red giant atmospheres of line formation, small-scale velocity fields, and convective motions; 2) estimate occurence of surface features like spots and active regions in red giants; and 3) derive rotation ($v \sin i$) and limb darkening in the bulge population of red giants. The imaging of spots and active regions suffers from degeneracies similar to those in Doppler imaging. However the ability of microlens imaging to resolve center-to-limb variations in spectral lines is exceptional and unique. So is the value of such information to the construction of a new generation of giant model atmospheres.

Discussion

M. Cuntz: I am a little bit concerned about the non-uniqueness of parameter fits of spots, if they exist (size, position, temperature of the spot). Do you see any way to improve that situation?

D. Sasselov: Yes, due to the degeneracy of the point lens microlensing problem, the reconstruction of surface features on the surface of the source is incomplete. One way out is by increasing the number of "observers" to two or more (e.g., space probes in the Solar system), which breaks some of the degeneracies. However, currently imaging by microlensing will provide only information on the occurence and filling factors of spots. Where the real strength of imaging by microlensing lies is center-to-limb variations, especially of spectral lines (and their profiles), which can provide unprecedented depth information. In this case, all the information can be recovered from the observations and the degeneracy does not matter.

References

Alcock, C., et al. 1997, ApJ, 491, 436

Allard, F., & Hauschildt, P., 1995, ApJ, 445, 433

Armstrong, J.T., et al. 1995, Physics Today, 48, 42

Canuto, V.M., Goldman, I., & Mazzitelli, I. 1996, ApJ, 473, 550

Dravins, D. 1990, A&A, 228, 218

Heyrovsky, D., & Loeb, A. 1997, ApJ, 490, 38 (astro-ph/9702097)

Heyrovsky, D., Loeb, A., & Sasselov, D. 1997, in Variable Stars and the Astrophysical Returns of Microlensing Surveys, eds. R. Ferlet, J.P. Maillard, & B. Raban (Gif sur Yvette: Editions Frontieres), 417

Heyrovsky, D., Sasselov, D., & Loeb, A. 1997, in preparation

Gould, A. 1992, ApJ, 392, 442

Gould, A. 1994, ApJ, 421, L71

Gould, A. 1995, ApJ, 441, L21

Gould, A., & Welch, D. 1996, ApJ, 464, 212

Kurucz, R.L. 1990, in Atomic Spectra for Astroph. & Fusion, ed. J.E. Hansen, North-Holland, 20

Kurucz, R.L. 1992, in Stellar Population of Galaxies, eds. B. Barbuy, & A. Renzini (Dordrecht: Kluwer), 225

Kurucz, R.L. 1997, in Fundamental Stellar Properties: The Interaction between Observation and Theory, eds. T.R. Bedding, et al. (Dordrecht: Kluwer), (CfA preprint 4571)

Loeb, A., & Sasselov, D.D. 1995, ApJ, 449, L33

Magain, P. 1986, A&A, 163, 135

Maoz, D., & Gould, A. 1994, ApJ, 425, L67

Nemiroff, R.J., & Wickramasinghe, W.A.D.T. 1994, ApJ, 424, L21

Nordlund, A., & Dravins, D. 1990, A&A, 228, 155

Paczyński, B. 1986, ApJ, 304, 1

Pont, F. 1997, in IAU General Assembly — JD14, Kyoto

Reid, I.N. 1997, in IAU General Assembly — JD14, Kyoto

Salaris, M., Degl'Innocenti, S., & Weiss, A. 1997, ApJ, 484, 986

Sasselov, D.D. 1996, in ASP Conf. Ser. 109, The Ninth Cambridge Workshop on Cool Stars, Stellar Systems and the Sun, eds. R. Pallavicini & A.K. Dupree (San Francisco: ASP), 541

Sasselov, D.D. 1997a, in Variable Stars and the Astrophysical Returns of Microlensing Surveys, eds. R. Ferlet, J.P. Maillard, & B. Raban, Editions Frontieres, 141

Sasselov, D.D. 1997b, in Fundamental Stellar Properties: The Interaction Between Observation and Theory, eds. T.R. Bedding et al. (Dordrecht: Kluwer), 253 (astro-ph/9705023)

Schwarzschild, M. 1975, ApJ, 195, 137

Simmons, J.F.L., Newsam, A.M., & Willis, J.P. 1995, MNRAS, 276, 182

Uitenbroek, H., Dupree, A.K., Gilliland, R.L. 1998, in ASP Conf. Ser. 154, The Tenth Cambridge Workshop on Cool Stars, Stellar Systems and the Sun, eds. R.A. Donahue & J.A. Bookbinder (San Francisco: ASP), 393

Valls-Gabaud, D. 1997, MNRAS, in press (astro-ph/9708098)

Vandenberg, D., & Bell, R.A. 1985, ApJS, 58, 561

Vandenberg, D. 1997, in IAU Symp. 189, Fundamental Stellar Properties: The Interaction Between Observation and Theory, eds. T.R. Bedding, A.J. Booth, & J. Davis (Dordrecht: Kluver), 439

Witt, H.J., & Mao, S. 1994, ApJ, 430, 505